RSC Sustainability

ROYAL SOCIETY OF CHEMISTRY

PAPER

View Article Online
View Journal | View Issue

Check for updates

Cite this: *RSC Sustainability*, 2024, **2**, 3123

Clay mineral-based sustainable snow contaminant remediation technology†

Benilde Mizero, [a] Saba Naderi,[a] Sandeep Bose, [a] Houjie Li [a] and Parisa A. Ariya*[ab]

Seasonal snow covers up to 33% of the Earth's surface. Fresh falling snow serves as a snapshot of atmospheric processes and can take up pollutants. Once deposited, snow can affect the Earth's radiation and climate change, and its melting and accumulation processes can affect human health. Little has been done for snow pollution remediation, especially regarding emerging materials and nano/microplastics in urban regions. We present a sustainable, cost-effective snow remediation filtering system made of multilayer clay-based minerals, specifically kaolin and montmorillonite, capable of removing nano/micro-contaminants from snow. In addition, a recycled metallic mesh with various pore sizes, including nano/micro size, can remove substantial snow contaminants. Using a suite of technologies including high-resolution S/TEM, Pelletier ice nucleation counter, NALDI mass spectrometry, Photoacoustic Extinctiometer (PAX), triple quad ICP-MS/MS, and TOC counter, we found that the clay-mineral setup is highly efficient. For instance, it removes metallic species (>95%), plastic micro/nanoparticles like polyethylene glycol and polyethylene (>99%), black carbon (>93%), and total organic carbon (>50%) from dirty snow sampled in the primary snow depository in downtown Montreal. This sustainable and inexpensive method is promising for significantly reducing the environmental impact of snow pollutants, improving current snow remediation practices in urban areas, decreasing the re-emission of contaminants in air, soil, and water leaching, and improving the ecosystem and human health.

Received 3rd April 2024
Accepted 12th September 2024

DOI: 10.1039/d4su00155a

rsc.li/rscsus

Open Access Article. Published on 23 September 2024. Downloaded on 2/21/2026 12:45:27 PM.
This article is licensed under a Creative Commons Attribution-NonCommercial 3.0 Unported Licence.

Sustainability spotlight

This research addresses the critical issue of snow pollution, particularly in urban areas, where snow acts as a repository for a variety of pollutants, including black carbon particles, nano/microplastics and metals. This pollution not only impacts environmental health but also affects human well-being. Our innovative snow remediation technique, utilizing clay-based materials, offers a sustainable and cost-effective solution to this pressing problem. The technology effectively removes a broad spectrum of contaminants, thereby improving snow purity and reducing potential re-emission into the environment. Aligning with UN SDG 6 (Clean Water and Sanitation), SDG 11 (Sustainable Cities and Communities), and SDG 12 (Responsible Consumption and Production), our approach contributes to reducing water pollution, enhancing urban environmental quality, and promoting sustainable waste management practices.

1 Introduction

The majority of the Earth's freshwater (80%) is stored in ice.[1] A significant portion of the cryosphere consists of permanently frozen or land-based ice masses, primarily located in Antarctica and Greenland, accounting for 2.1% of the Earth's water reserves.[2] Conversely, a substantial portion of the globe experiences seasonal snow, leading to seasonally frozen ground characterized by high variability in areal extent. The most extensive coverage occurs during the winter season, encompassing up to 62% of the Eurasian continent and nearly all North America.[2,3] The interaction between frozen ground and solar radiation makes snow and ice-covered surfaces significant contributors to Earth's radiative energy balance, influencing climate and temperature regulation.[4] Snow is particularly crucial due to its high albedo, which allows it to reflect a large portion of sunlight. However, the presence of impurities can significantly alter snow's albedo. Absorptive impurities like black carbon reduce the snow's reflectivity,[5] leading to increased solar radiation absorption and faster snowmelt. Additionally, these impurities affect the formation and size of snow grains, with larger grains decreasing the surface-to-volume ratio, further lowering the snow's albedo.[6] Thus, impurities affect how sunlight is reflected and absorbed and

[a]*Department of Chemistry, McGill University, Montreal, Quebec H3A 0B8, Canada. E-mail: parisa.ariya@mcgill.ca*

[b]*Department of Atmospheric and Oceanic Sciences, McGill University, Montreal, Quebec H3A 0B9, Canada*

† Electronic supplementary information (ESI) available. See DOI: https://doi.org/10.1039/d4su00155a

© 2024 The Author(s). Published by the Royal Society of Chemistry

Open Access Article. Published on 23 September 2024. Downloaded on 2/21/2026 12:45:27 PM. This article is licensed under a Creative Commons Attribution-NonCommercial 3.0 Unported Licence.

impact the snow grain structure, ultimately influencing the albedo and contributing to climate change.[6]

Snow manifests in diverse types, each with distinct climate effects.[2] Two primary types are distinguished based on water content: dry snow, characterized by low water content and a high albedo, contribute to cooling the Earth's surface as it reflects a significant portion of incoming solar radiation. Dry snow predominates in cold, high-latitude regions and mountainous areas.[3] In contrast, wet snow, marked by high water content and density, has a lower albedo than dry snow, absorbing more solar radiation and potentially causing localized warming. Wet snow is common in regions with milder winter temperatures.[7,8] Besides water content, other factors influencing the snow type include temperature, anthropogenic/industrial activities, geographical location, and elevation. Arctic snow, known for being cold and dry, accumulates significantly at extremely cold temperatures.[9] Alpine snow varies with elevation and temperature, exhibiting a mix of wet and dry snow.[10,11] Urban snow, influenced by human activities, undergoes frequent freeze–thaw cycles, may be contaminated with pollutants, and often becomes denser due to foot and vehicle traffic.[12] Moisture content ranges from drier in the Arctic region to variable levels in Alpine areas and is influenced by local sources in urban regions. The colour differs, with urban snow appearing dirtier, while Arctic and Alpine snow tend to be whiter and purer. It is evident that the impact of these snow types on climate change, through particle emission and Earth radiation, varies significantly.[2,3]

Numerous environmental studies show that natural phenomena and anthropogenic activities are responsible for releasing airborne particles of various sizes, chemical compositions, physical properties and phases.[13–16] The high absorption capacity of snow/ice, combined with the provision of an ideal photochemical environment and conditions for particles to react and form new molecules expands the physicochemical spectrum of particles found in the snow/ice medium.[17–20] Some of the latter particles are inorganic molecules such as common, precious, and rare earth metals, ionic compounds,[18,21,22] organic compounds (*e.g.*, pollen,[23] plastic fragments,[24,25] polycyclic aromatic compounds (PAHs),[26,27] pesticides,[28] and volatile organic compounds[20,29–31]), biological molecules including proteins, peptides, nucleic acids, as well as some biological entities namely bacteria, viruses, and fungi,[32–36] trace gases (SO_2, Hg, *etc.*)[37], and light-absorbing carbonaceous particles (brown carbon and black carbon).[38,39]

Although there are snow-borne molecular compounds with low toxicity, some of the particles found in the snow medium, like pesticides and PAHs, nano/microplastics (*e.g.*, polyethylene, or polystyrene) and metallic species (*e.g.*, Cr and Ni), have been shown to have adverse health effects and downgrade the air quality.[40–42] They have been associated with respiratory complications (*e.g.*, pneumonia and asthma attacks),[43,44] cardiovascular issues, encephalopathy, nephrotoxicity, bone damage and dyslexia.[45] Annual statistical reports released by the World Health Organization in the past years indicate 7 million premature deaths linked to air pollution.[46,47] Additional alarming data show that in 2019, 99% of the world's population lived in areas that did not meet the 2021 air quality guidelines set by the WHO.[48]

The impact of the snow-borne particles on climate change is also not negligible. The influence on environmental and climate changes occurs at different levels including, but not limited to the disturbance of the Earth's hydrological cycle by impacting the natural occurrence of precipitation through processes such as cloud formation and ice nucleation, as well as disturbing the Earth radiative energy balance through scattering, absorption, and diffusion of terrestrial and solar radiation by light-absorbing carbonaceous particles.[13]

The snow-adsorbed particles can be released back into the atmosphere during snow's precipitation, melting and evaporation cycles. Furthermore, they can leach into the soil or reach the aquatic system through melted water run-offs, especially if they are water-soluble.[13,19,28,42,49,50] Consequently, there is a growing concern regarding snow released airborne particles, hence, stressing the need to explore and develop technologies of snow decontaminations.

Over the past few years, numerous techniques have been developed to remove impurities from stormwater/wastewater that are/can be used for snowmelt decontamination to ensure that the melted snow or runoff is cleaner and safer for the environment. Table 1 depicts some of these remediation techniques. Most of the current methods are characterized by narrow molecular selectivity, extensive labor and cost for installation/maintenance, high energy consumption, and greenhouse gas emissions (thus contributing to climate change) and are effective only for larger macro particles; research shows that the majority of the particles found in snow are nanosized.[61] In this study, our goal is to develop a novel technology to remove a wide range of small particles (micro/nanoscale) using natural clay minerals, with additional sustainable recycling.

2 Experimental

2.1 Snow collection procedure

Accumulated-aged snow samples were collected close to the bottom surface at McGill University and a Montreal snow deposit site, stored in pre-sterilized amber glass bottles, and kept in the dark and frozen immediately, until chemical analysis.

2.2 Filtration set up for purification

The collected snow was allowed to melt at room temperature and transferred in a separating funnel to control the dripping rate (maintained to about 1 drop per second). Below the funnel, we positioned a Buchner funnel containing different filtering layers. Each layer was made by evenly spreading about 10 g of clay material on an 11 μm pore size paper filter. At the bottom of the funnel, a vial was positioned to collect the filtrate. We determined that at least 10 grams of clay was necessary to fully cover the surface of the filter paper, ensuring that all the melted snow water would pass through the filter effectively. This is why we opted to use 10 grams of clay in our setup. The prepared samples include non-clay filtered (filtration achieved through

 © 2024 The Author(s). Published by the Royal Society of Chemistry

Open Access Article. Published on 23 September 2024. Downloaded on 2/21/2026 12:45:27 PM. This article is licensed under a Creative Commons Attribution-NonCommercial 3.0 Unported Licence.

Table 1 Survey of common decontamination techniques used for precipitation water treatment

Decontamination technique	Methodology description	Limitations	Targeted contaminants
Physical filtration, sedimentation basins	Placement of mesh screens, sediment fences, oil/grit separator in the path of snowmelt to remove pollutants	Failure to target nanoparticles	Larger particles and debris[51]
Bioretention and bioswales	Use of vegetation and engineered soils to remove pollutants	Climate sensitivity High initial building cost Design challenges	Large, suspended solids[52] Metallic species[53] Soluble phosphorous[54] Microplastics[55]
Activated carbon filters	The unfiltered sample is passed through a filter containing the adsorbents	Limited selectivity	Trace organic compounds Metallic species[56]
Coagulation/flocculation processes	Addition of chemical coagulants or flocculants can be added to melted snow to promote the clumping of small particles before filtering them out	Limited selectivity Necessity of additional filtration technique	Natural organic matter[57]
Electrocoagulation	Electrochemical treatment process which uses soluble anodes made of coagulating metals to destabilize and aggregate contaminants	Limited selectivity Necessity of additional filtration technique	Natural organic matter[58]
Ultraviolet (UV) treatment	Used to disinfect melted snow by exposing it to ultraviolet light	Limited selectivity Production of toxic waste	Microorganisms[59]
Reverse osmosis	A semi-permeable membrane and pressure are used to retain the contaminants	Expensive Energy intensive Not ideal for large scale snow filtration	All contaminants[60]

an 11 μm pore size filter paper), kaolin filtered, montmorillonite filtered, kaolin–montmorillonite composite (using 5 grams of each) as well as kaolin–magnetite–montmorillonite composite (the layers were separated by a filter paper). As we wanted to focus on assessing the ability of the clay materials to remove nanoparticles, the sample was filtered through a 200 nm pore size filter prior to the chemical analysis. The following steps involved analyzing the samples through a range of rigorous analytical techniques targeting specific pollutants as depicted in Fig. 1. An additional filtration setup was assembled comprising different layers, starting with large grid size metallic meshes (from decimeter to millimeter pore size diameters) followed by clay powder in an cotton bag with a 38 micrometer grid size metallic (Fig. S1†) mesh to mimic a system proposed to scale up the clay remediation process for urban snow deposit sites.

2.3 Qualitative and quantitative analysis

2.3.1 Droplet freezing assay. Before each analysis, the samples were sonicated for 20 minutes. Subsequently, a thin layer of petroleum jelly was spread on an in-house-made copper cooling plate, thus creating a hydrophobic layer, and minimizing the influence of the copper plate on the freezing process. For each sample, 200 droplets of 10 μl each were carefully placed and evenly distributed in groups of 50 at each corner of the square plate. Starting at a temperature of around 0 °C, the chamber was cooled at a rate of 1 °C min^{-1}. The temperature at which each droplet froze was observed by the naked eye and recorded (the accuracy of this step was ensured by videotaping the whole experiment and re-watching the video to assess the freezing temperature of each droplet).

Because the nucleation process was assumed to occur by immersion in a supercooled droplet, comparison was made by the quantification of active site density per unit mass. The cumulative number of ice nucleation active sites per unit volume of water (K) at a certain temperature (T) is obtained from eqn (1).

$$K(T) = \frac{-\ln(1 - f_{ice})}{V} \quad (1)$$

where f_{ice} is the fraction of frozen droplets and V is the volume of the droplet. Given the mass of particles per unit volume of water determined, the ice nucleation active site density per unit mass (n_m) can also be expressed according to eqn (2).

$$n_m(T) = \frac{K(T) \times d}{C_m} \quad (2)$$

where C_m represents the mass concentration of the particles in the initial suspension, while d represents the dilution ratio of the suspension relative to C_m. Lastly, the mean freezing temperature for each sample was calculated and reported.

For each filtration sample, 360 data points were collected across three runs, with each run consisting of 120 data points. The mean freezing temperature was calculated for each run, and the standard error was computed to account for variations between the trials. These variations are represented as error bars in the results.

2.3.2 Metal analysis. For this part, the sample preparation was conducted following the US Environmental Protection Agency method 200.8 (EPA 200.8) for total recoverable elements

Open Access Article. Published on 23 September 2024. Downloaded on 2/21/2026 12:45:27 PM.
This article is licensed under a Creative Commons Attribution-NonCommercial 3.0 Unported Licence.

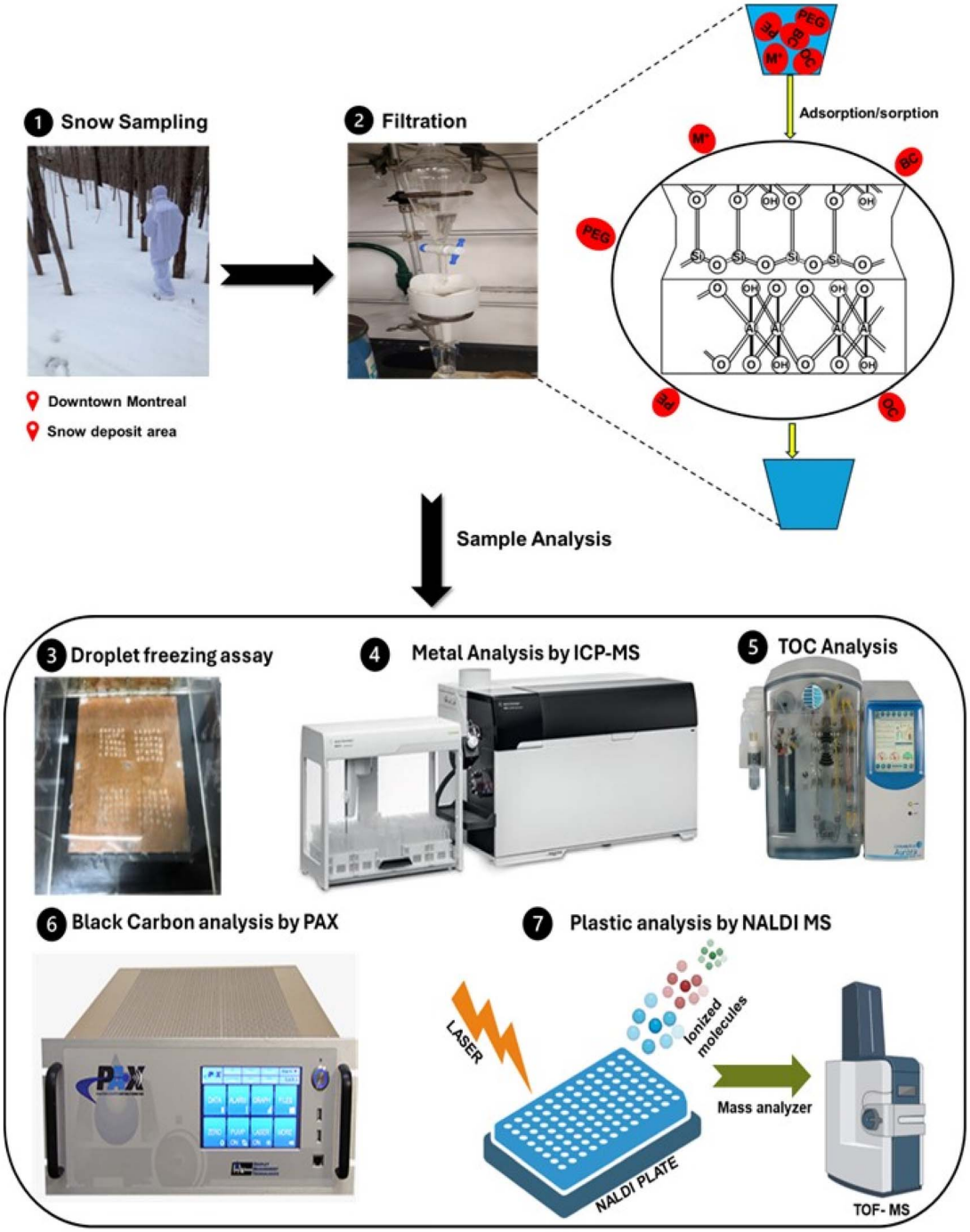

Fig. 1 Experimental workflow encompassing the filtration system along with the molecular targeted analytical techniques for snow-borne particles.

in aqueous samples. The preparation started with acidification of about 100 ml of each sample with (1 + 1) a nitric acid solution to pH < 2 (300 µl of acid was added); the samples were then rested for at least 16 hours and the pH was verified to be less than 2. The next step was a digestion process achieved by adding 2 ml (1 + 1) of nitric acid and 1.0 ml (1 + 1) of hydrochloric acid in the sample and gently heating it at 85 °C for about 2 hours until the volume was reduced to 20 ml. The sample was then refluxed for about 30 minutes, cooled to RT, and diluted to 50 ml with reagent water (1% nitric acid in Milli-Q water v/v) prior to centrifugation to get rid of undissolved solids. The next step aimed to further reduce the chloride concentration by pipetting 20 ml of the supernatant and diluting it to 50 ml with reagent water. Lastly, the digested samples were filtered through a 0.45 µm pore diameter membrane filter before being injected into a 8900 ICP-MS Triple Quad (Agilent).

© 2024 The Author(s). Published by the Royal Society of Chemistry

Open Access Article. Published on 23 September 2024. Downloaded on 2/21/2026 12:45:27 PM. This article is licensed under a Creative Commons Attribution-NonCommercial 3.0 Unported Licence.

We used Ar as the plasma gas; the nebulizer pump speed was set at 0.3 rps with a 45-second long sample uptake. The data were acquired in four different reaction modes (no gas, H_2, O_2 and NH_3) using the spectrum acquisition mode with the options of 1 point for Q2 peak pattern, 3 replicates and 20 sweeps/replicate.

To correct for instrument drift and physical interferences, a water-based solution of indium (1 ppm) was used in all analyses by mixing it with the analyte solution prior to nebulization, using a different channel of the peristaltic pump and a mixing coil.

To achieve quantification, a stock solution of Ag, Al, As, Ba, Be, Cd, Co, Cu, Cr, Mn, Ni, Pb, Sb, Se, Sr, Th, Ti, Tl, U, V, and Zn (10 mg l^{-1}) and Fe, Mg, K, Na, and Ca (1000 mg l^{-1}) in water reagent was first prepared and diluted 10^3, 10^4 and 10^5 times corresponding to 3 levels of calibration standards.

For the ICP-MS/MS results, quality control and instrumental error tracking were conducted by injecting mixtures of known concentrations. Two trials were performed, and the results are provided in Table S2.†

2.3.3 Analysis of total organic compounds. Samples were analyzed with an OI Analytical Aurora 1030W TOC analyzer using a persulfate oxidation method at the GRIL-Université du Québec à Montréal (UQAM) analytical laboratory. The calibration was performed as follows: 8 ml of water was subsampled from each sample. 0.5 ml of 5% phosphoric acid was added to the subsample and combusted at 70 °C, to detect total inorganic carbon. Afterwards, 3 ml of 10% sodium persulfate was added and combusted at 98 °C to detect organic carbon. The resulting CO_2 from these two reactions was then detected separately using a nondispersive infrared sensor (NDIR). Each sample was processed in duplicate. Internal standards (0 and 5 ml l^{-1} DOC) and external standards (5 mg l^{-1} DOC) were included in each batch of samples to ensure the consistency of results between each analysis.

2.3.4 Qualitative and quantitative analysis of plastic. For polyethylene glycol (PEG) analysis, a stock solution of 40 mg l^{-1} was prepared by dissolving 20 mg of polyethylene glycol of $M_w \sim$ 1000 (PEG-1000) in 500 ml of Milli-Q water, mixed and gently shaken at 110 rpm for 24 h. The latter solution was then diluted to make five standard solutions with concentrations of 0.01, 0.025, 0.05, 0.3 and 0.5 mg l^{-1}.

For polyethylene analysis, we started by making a solution of 10 mg ml^{-1} polyethylene of $M_w \sim$ 800 (PE-800) in toluene by heating the mixture for an hour at 85 °C. We spiked 2 ml of the latter solution in 10 ml of melting snow water, followed by one-hour sonication. The sample was deposited right after sonication on the MALDI plate.

Lastly, a suspension of ZnO (1% wt.) in methanol and a saturated solution of $AgNO_3$ in ethanol were then prepared and sonicated for at least 30 minutes before the analysis. To achieve nanostructure laser desorption ionization, the saturated salt solution and the metal oxide suspension solution were mixed with the standard solution or the sample in a 1 : 10 : 20 ratio and 1 μl of the mixture was deposited and air dried on a stainless steel MALDI plate (Bruker). The plate was immediately inserted into an Autoflex III MALDI TOF mass spectrometer (Bruker) controlled by Flex Analysis 3.4. The system was operated in reflectron positive ion mode, with an acceleration voltage of 18.8 kV. The ionization source was a 355 nm frequency tripled Nd:YAG SmartBeam™ laser (Bruker).

Four distinct spots were created on the plate for each sample by depositing 1 μl of the sample, which was then air-dried. The laser was pulsed 200 times on each spot to obtain a spectrum. Multiple spectra (4 spots × 200 shots) were integrated to produce a composite spectrum for each sample. This composite spectrum was then used to determine the concentration. The experiment was repeated three times for each sample to account for run-to-run variation.

2.3.5 Black carbon analysis. To measure changes in Black Carbon (BC) mass concentration, a Photoacoustic Extinctiometer (PAX) was utilized. Detailed information about PAX is available elsewhere.[39] In summary, the PAX samples air at a flow rate of 1 liter per minute. It features a laser with a wavelength of 870 nm that passes through its absorption chamber. Notably, it is assumed that only BC absorbs the light at this wavelength.[39] When BC particles absorb this light, they heat up, transferring the heat to the surrounding air. This process generates periodic sound waves, which are then detected by a sensitive microphone inside the chamber. By analyzing these sound waves, the absorption coefficient of BC is determined. Given that the mass absorption cross-section of BC is 5 m^2 g^{-1}, the mass concentration of BC can be calculated by dividing the absorption coefficient by the mass absorption cross-section.

For the BC determination experiment, the samples needed to be aerosolized before being injected into the PAX. Hence, each sample was collected into a 15 ml plastic syringe and positioned into a syringe pump set at a flowrate of 0.25 ml min^{-1}; a connector was used to connect the outlet of syringe with the outlet of an air tank to achieve nebulization and then directed into a silica bead diffusion dryer, directly connected to the analytical instrument. The air pressure from the tank was set to achieve a flowrate of 0.95 l min^{-1} in the PAX. The concentration of BC was measured every second for five minutes.

The average concentration was calculated for each trial, with the average Milli-Q water value subtracted to account for instrument background. Each sample was analyzed in three trials, and the results were used to calculate the standard error.

2.3.6 High-resolution electron microscopy. Scanning/Transmission Electron Microscopy (STEM) with a High-Angle Annular Dark Field detector (HAADF) was employed to capture images of particle structures using a TALOS F200X transmission electron microscope (Thermofisher, USA). Energy-dispersive X-ray spectroscopy (EDS) maps were generated with a 700 pA current beam in STEM mode. For sample preparation, two types of grids (a glow-discharged silicon oxide-coated copper electron microscopy grid and a gold TEM grid with carbon as the substrate) were employed, onto which a 10 μl solution of our sample was deposited. The liquid was allowed to evaporate at room temperature.

2.3.7 Electrochemical mediated regeneration of used clay minerals. This section of our experimental procedure aimed to regenerate the adsorption ability of the clay mineral by

Open Access Article. Published on 23 September 2024. Downloaded on 2/21/2026 12:45:27 PM. This article is licensed under a Creative Commons Attribution-NonCommercial 3.0 Unported Licence.

subjecting it to electrolysis. 10 g of montmorillonite was collected post-remediation and 200 ml of ultra-purified Milli-Q water was added, followed by a five-minute sonication. NaCl was chosen as the electrolyte, with 4 g added to the mixture. A DC power supply was used to apply a potential of 12.0 V (current ∼ −0.4 A). Two types of electrolysis were conducted depending on the electrodes used: the first one was conducted using copper wires as both the cathode and anode, whereas, in the second one, pieces of graphite isolated from a pencil were used. The electrochemically mediated clay regeneration was tested by comparing the elemental analysis (ICP-MS) of small aliquots sampled before and after the electrolysis.

2.4 Materials and supplies

All the reagents used were of analytical reagent (AR) grade, and Milli-Q water was used throughout the experiment. Kaolin powder (PCode: 1003167143) and montmorillonite powder (PCode: 102372473) were purchased from Sigma Aldrich. Polyethylene glycol with $M_w \sim 400$ (PEG-400) and ZnO powder (40–100 nm) were purchased from Thermo Fisher Scientific. The acidic solutions used for ICP-MS analysis were trace metal grade and purchased from Sigma Aldrich.

3 Results and discussion

3.1 Snow samples

Our goal was to investigate the ability of clay materials to remove pollutants from snow water. The investigation was conducted by comparing snow samples before and after the remediation process; different samples were collected, and the concentration of various chemical particles was determined and compared. About eight different samples were made depending on the analytical process: untreated snow (unfiltered), snow filtered with an 11 μm pore size paper filter, snow filtered with two types of clay separately (montmorillonite and kaolin), a combination of both clay minerals, and ultra-purified water with 18.2 Mω·cm conductivity (Milli-Q) used as a standard and to get an idea of the purity of our remediated snow samples.

3.2 Ice nucleation analysis

Inspired by the well-established correlation between particle concentration in water and its proclivity to freeze at higher temperature than its intrinsically freezing point when in its purest form; we conducted droplet freezing assays for each of our samples. The nucleation ability can be assumed because of the wide range of physicochemical variability among particles dissolved in water, thus reducing the impact of individual contribution of the chemical identity of each particle.

The comparison of the mean freezing temperatures from the droplet freezing assay can serve as an early indicator of the success of the remediation procedure. The results of the mean freezing temperatures (MFT) in decreasing order are −11.41 °C (−4.1 to −14.7 °C), −13.43 °C (−6.9 to −15.1 °C), −16.94 °C (−7.4 to −20.8 °C), −16.46 °C (−8.5 to −18.9 °C), −16.09 °C (−6.9 to −18.9 °C) and −19.86 °C (−4.1 to 24.5 °C) for the raw sample (unfiltered), the 11 μm filter-filtered, the montmorillonite-filtered, the Kaolin-filtered, the kaolin–montmorillonite combination-filtered and the Milli-Q samples, respectively (Fig. S2†). Lowering the MFT after filtration with an 11 μm pore size filter paper fortifies the earlier mentioned hypothesis of the negative correlation between the cleanliness of the water and its MFT. The MFT was even lower for the clay samples, providing initial insights into their ability to bind particles dissolved in snow water and remove them (Fig. S2†).

The MFT for the clay remediated samples was similar, with montmorillonite showing the lowest temperature compared to the other ones. That said, it does not clearly indicate that it is a better filtering material than Kaolin because not only the difference is minimal but also one could argue that it might be due to the nature of the freezing assay that is mainly directed toward the immersion freezing process, considerably reducing the contribution of other nucleation modes (*e.g.*, deposition, condensation and contact freezing). Additionally, and most importantly, montmorillonite could be a better adsorbent of particles with a higher nucleation ability than Kaolin. Hence, a deeper analysis is needed based on the chemical identity of the particles found in snow water.

3.3 Assessment of clay mediated remediation at the elemental level: focus on metallic species

Environmental pollution associated with metal particles has been shown at different levels and is related to both climate change and health issues.[62,63] For instance, heavy metal ions exhibit a high toxicity to living organisms, mainly through oxidative damage. They can interact with biomolecules and change their structural conformation, concomitantly, their biological functions.[64] With the expansion of the metal mining and transformation industries, the emission of metal pollutants is becoming increasingly concerning. Thanks to technological advancements, we can now analyze metal elements at the nanoscale level, highlighting their negative influence on the environment. For this, we had to investigate the ability of clay to remove metal pollutants in snow medium. The concentration of different elements in our samples was determined using an ICP-MS analytical device. To evaluate the clay-mediated metal uptake, we calculated the removal percentage of each component by dividing its concentration in the remediation sample by its concentration in the unfiltered sample. These values are all reported in Table 2. Additionally, mapped HAADF images showed the presence of most of the abundant metallic elements depicted in Table 2, as shown in the ESI.†

Our study revealed that iron is one of the most prevalent metals in snow, with its concentration significantly reducing from 3464.23 μg l^{-1} in the unfiltered sample to 8.49 μg l^{-1}, 58.02 μg l^{-1}, and 37.40 μg l^{-1} in samples filtered with kaolin, montmorillonite, and a combination of both, respectively. These values correspond to removal efficiencies of 99.76%, 98.33%, and 98.92%, respectively. Aluminium, another metal found in high concentrations, resulted in a removal efficiency of nearly 95% for the kaolin-filtered sample. Additionally, metals such as Pb, Ti, Cr, U, Zn, and vanadium were effectively removed by both clay materials, with at least an 80% reduction. Generally,

© 2024 The Author(s). Published by the Royal Society of Chemistry

Open Access Article. Published on 23 September 2024. Downloaded on 2/21/2026 12:45:27 PM.
This article is licensed under a Creative Commons Attribution-NonCommercial 3.0 Unported Licence.

Table 2 Mass concentration of metal ions for the analyzed samples and assessment of the metal uptake by calculating the percentage of the concentration of the filtered samples compared to the unfiltered ones

	Tap	Milli-Q	Unfiltered	Kaolin		Montmorillonite		Kaolin–montmorillonite	
Element	[μg l^{-1}]	[μg l^{-1}]	[μg l^{-1}]	[μg l^{-1}]	Removal%	[μg l^{-1}]	Removal%	[μg l^{-1}]	Removal%
Fe	8.86	0.66	3464.23	8.49	99.76	58.02	98.33	37.40	98.92
Pb	0.81	0.01	29.54	0.15	99.48	0.42	98.57	0.45	98.49
Ti	0.28	0.26	127.96	3.54	97.24	4.31	96.63	3.26	97.45
Cr	0.10	0.04	12.06	0.36	96.97	0.43	96.44	0.47	96.10
Th	<0.00000	<0.00000	0.20	0.01	95.44	0.03	83.29	0.03	86.67
Al	14.23	2.76	2552.32	136.22	94.66	887.44	65.23	381.61	85.05
U	0.30	<0.00000	0.31	0.04	88.50	0.18	42.16	0.18	42.09
Zn	63.30	2.34	121.06	16.18	86.83	23.72	80.41	18.83	84.45
V	0.13	0.00	9.06	1.79	80.28	0.06	99.33	1.46	83.87
Mg	8012.17	0.85	6834.11	1590.46	76.73	7295.51	0.00	3163.44	53.71
Mo	1.06	<0.00000	3.07	0.92	70.06	0.01	99.58	0.18	94.19
Mn	0.60	ND	98.75	33.55	66.03	50.48	48.88	41.96	57.51
Cs	0.00	<0.00000	0.31	0.11	64.84	0.31	0.93	0.21	33.47
Sb	0.16	0.00	1.30	0.50	61.57	0.06	95.93	0.30	76.88
As	0.44	<0.00000	1.66	0.75	54.68	1.51	8.91	2.04	0.00
Ba	23.36	0.06	26.44	13.46	49.09	15.09	42.91	15.47	41.49
Ca	28529.22	27.34	75556.38	39590.37	47.60	30425.33	59.73	34356.20	54.53
Si	1165.04	618.19	11476.83	6042.95	47.35	10687.61	6.88	8719.37	24.03
Ni	3.57	0.05	9.83	5.38	45.26	4.74	51.74	8.54	13.10
Sr	172.39	0.09	872.96	478.35	45.20	258.42	70.04	361.83	58.55
Cd	0.01	<0.00000	0.18	0.10	42.13	0.06	67.79	0.15	14.71
Rb	1.00	ND	3.80	2.96	21.99	19.70	0.00	6.67	0.00
Li	1.89	0.02	3.93	3.08	21.45	52.12	0.00	37.09	0.00
Co	0.02	0.00	1.69	1.65	2.18	1.02	39.43	2.54	0.00
K	1423.43	1.95	829.70	836.35	0.00	3141.18	0.00	1645.75	0.00
S	6806.79	4.45	46335.59	59239.54	0.00	45809.18	1.14	53704.39	0.00
Be	<0.00000	<0.00000	0.10	0.13	0.00	0.34	0.00	0.48	0.00
Cu	717.66	1.70	31.03	47.36	0.00	10.42	66.41	59.26	0.00
Tl	<0.00000	<0.00000	0.01	0.05	0.00	0.08	0.00	0.07	0.00
Na	16211.87	10.83	3392.58	32080.54	0.00	13861.84	0.00	29690.12	0.00
Se	0.07	<0.00000	0.07	6.42	0.00	0.12	0.00	4.57	0.00

a high removal efficiency was observed for transition and post-transition metals compared to alkali and alkaline earth metals. Notably, sodium and potassium levels increased post-treatment in all clay-filtered samples, suggesting that they were released from the clays during the filtering process. To explore this further, control experiments were conducted by passing Milli-Q water through the filtration setup, and the resulting filtrate was analyzed to determine the concentration of leached metals. As shown in Table S4,† the results revealed a significant increase in concentrations, particularly for alkali and alkaline earth metals.

Regarding the effectiveness of the different types of clay minerals, kaolin generally showed superior metal sorption compared to montmorillonite, with magnesium serving as a prime example. Despite being prevalent in snow water, magnesium's concentration remained unchanged after montmorillonite treatment, whereas kaolin achieved about 77% reduction. However, montmorillonite was more effective in removing certain metals, like calcium, reducing its concentration by nearly 60%, compared to kaolin, which achieved a 48% reduction. Similarly, strontium removal was about 70% with montmorillonite and 45% with kaolin.

Based on the experiments conducted on snow from two sites (Downtown McGill and a designated disposal area), there was a notable difference in the concentrations of inorganic-metal contaminants, as shown in Table S3.† The metal concentration was significantly higher in the snow collected from the dump site than in the snow from the McGill downtown campus. Additionally, in terms of percentage removal, the removal efficiency was generally lower for the snow collected from the campus than from the dump site. This discrepancy is likely due to variations in the concentration levels of metal contaminants, the proximity of hotspot emissions, meteorological factors,[65] and the high prevalence of salts at the snow disposal sites.

The observed high metal uptake and the specific affinity to some of the metal pollutants are an outcome of the underlying physical and chemical properties of the clay materials as well as a combination and competition of different interaction mechanisms between clay minerals and the metal pollutants. The metal uptake is achieved through a combination of other mechanisms: ion exchange, surface complexation and surface precipitation.[66,67] All these mechanisms are highly specific to the molecular structure of the adsorbent and the adsorbed particle. For instance, the ion exchange will, to a certain degree,

Open Access Article. Published on 23 September 2024. Downloaded on 2/21/2026 12:45:27 PM. This article is licensed under a Creative Commons Attribution-NonCommercial 3.0 Unported Licence.

occur through an isomorphic substitution or by occupying empty interstitial sites in the clay structural unit cell, thus introducing a size dependency parameter.[66,67] This phenomenon is one the reasons why the uptake is high for transition metals, as they make up the central core of unit cells in clay materials.

Studies on the structural characterization of phyllosilicates show an elemental organization in tetrahedral and octahedral sheets, with each tetrahedron unit cell composed of a central cation (mostly Si^{4+}, Al^{3+} or Fe^{3+}) coordinated to 4 oxygen atoms (3 in the basal position and 1 in the apical position pointing up or down) that connect them to another tetrahedron by sharing the three-cornered basal oxygen to form an infinite hexagonal mesh pattern. The latter is also observed for octahedral organization where the central cation (usually, Al^{3+}, Fe^{3+}, Fe^{2+} or Mg^{2+}) is coordinated to six oxygen atoms connected into a two-dimensional hexagonal or pseudohexagonal sheet by sharing the peripheral edge atoms. Because of this unique orientation, some of the edges in octahedra are in the form of hydroxyl groups.[64–66]

The alternation of oxygen atoms and hydroxyl group plays an essential role in the overall crystal orientation, the layer charge, adsorption specificity and the affinity's strength to different molecules being absorbed/adsorbed. For example, in the kaolin group, the structural layer is achieved through the combination of a tetrahedral sheet (*T*) and an octahedral sheet (O) (1 : 1, TO layering). In contrast, montmorillonite's octahedral sheet is sandwiched between two tetrahedral sheets in a 2 : 1 TOT layering. This difference in structural formation has chemical and physical repercussions that might explain the discrepancies in metal ion affinity between kaolin and montmorillonite. One of the consequences of the 2 : 1 layering is the masking of the hydroxyl group through their interaction with the apical oxygen atoms of the tetrahedra on both sides of the sheets. More importantly, the size of the interlayer space varies along with its molecular content composition; for the TO assembly, it is mainly empty, whereas, for TOT, it is filled with alkali/alkaline earth metals and water molecules.[66–69] The latter differences further intensify the variability in metal affinity with kaolin and montmorillonite.

3.4 Assessment of clay mediated remediation for organic pollutants

3.4.1 Total organic compound (TOC) analysis. One of our previous studies focusing on identifying the particles in snow showed that TOC particles are present in both micro and nano sizes.[14] Other studies have shown different pathways, including metal-mediated pathways of forming secondary organic aerosols that contribute highly to the concentration of organic compounds in the snow medium.[70,71] Thus, in the remediation evaluation, we aimed to compare the TOC concentration in our samples before and after filtration. An additional filtration sample was created sandwiching a magnetite layer between kaolin and montmorillonite layers inspired by previously published studies on the adsorption of organic compounds on magnetite.[72–74]

The determined TOC concentrations for unfiltered, kaolin-filtered, montmorillonite-filtered, two layer combination (kaolin–montmorillonite)-filtered, three layer combination (kaolin–magnetite–montmorillonite)-filtered and milli-Q samples were 11.4, 5.6, 7.91, 7.39, 7.16 and 0.32 mg per samples, respectively. As per the results, kaolin depicted the highest absorption capacity for organic compounds with a decrease of about 51% compared to the unfiltered sample, a decrease that was even greater than that observed upon filtration with an additional magnetite layer (Fig. 2A). This improved affinity can be attributed to kaolin's unique molecular/atomic organization, discussed in the previous section.

Two main groups of substances that clay materials adsorb in TOC are biological/organic cations and non-ionic organic compounds. The mechanism of uptake of the former is attributed to the hydrophilic nature of the clay materials which allows a coulombic attraction to take place involving the charge transfer between the cation and the negatively charged silicate body appended to the cation exchange process. As for non-ionic compounds, the uptake can be associated with the large specific surface area and the porosity of the clay materials.[66,68,75]

3.4.2 Black carbon (BC) analysis. Black carbon (BC) has been a hot topic in environmental studies for quite some time now. Its effect on the disruption of the Earth's radiative energy has been profoundly investigated and proven.[76] As outlined in the Introduction, BC has a multifaceted impact on the climate. It directly warms the atmosphere by absorbing solar radiation. Indirectly, BC influences climate by acting as nuclei for cloud and snow formation, leading to either warming or cooling effects.[13,39,76,77] Additionally, when BC deposits on surfaces like snow, ice, and glaciers, it darkens them, hastening their melting.[78] This process reduces the snow's albedo (reflectivity), further contributing to climate warming.

The presence of BC in snowpacks has been extensively documented in both cryospheric and urban regions. To support this, we performed a high-resolution electron microscopy experiment on the unfiltered sample that yielded S/TEM images showing the structure of BC (Fig. 2, panel F). In addition, carbon-mapped HAADF images along with EDS results of unfiltered clay show a high propensity of C in the sample, thus confirming the presence of BC in the collected non-treated aged snow (Fig. 2, panels C–E). For this reason, BC was chosen as one of the focal points in this study.

To evaluate the ability of clay in removing BC from snow water, the filtered and unfiltered samples were aerosolized and tested for BC particles using a photoacoustic exctintiometer (PAX) to determine their concentration in the aerosolized volume. As shown in Fig. 2B, the results show that the particle concentration is lower for montmorillonite- and kaolin-filtered samples compared to the raw, unfiltered samples.

The effectiveness of montmorillonite and kaolin in removing BC particles can be attributed to several key factors associated with the properties of clay minerals:

(1) High surface area and adsorption sites:

Clay minerals, such as montmorillonite and kaolin, have high surface areas, providing numerous BC particle adsorption

© 2024 The Author(s). Published by the Royal Society of Chemistry

Open Access Article. Published on 23 September 2024. Downloaded on 2/21/2026 12:45:27 PM.
This article is licensed under a Creative Commons Attribution-NonCommercial 3.0 Unported Licence.

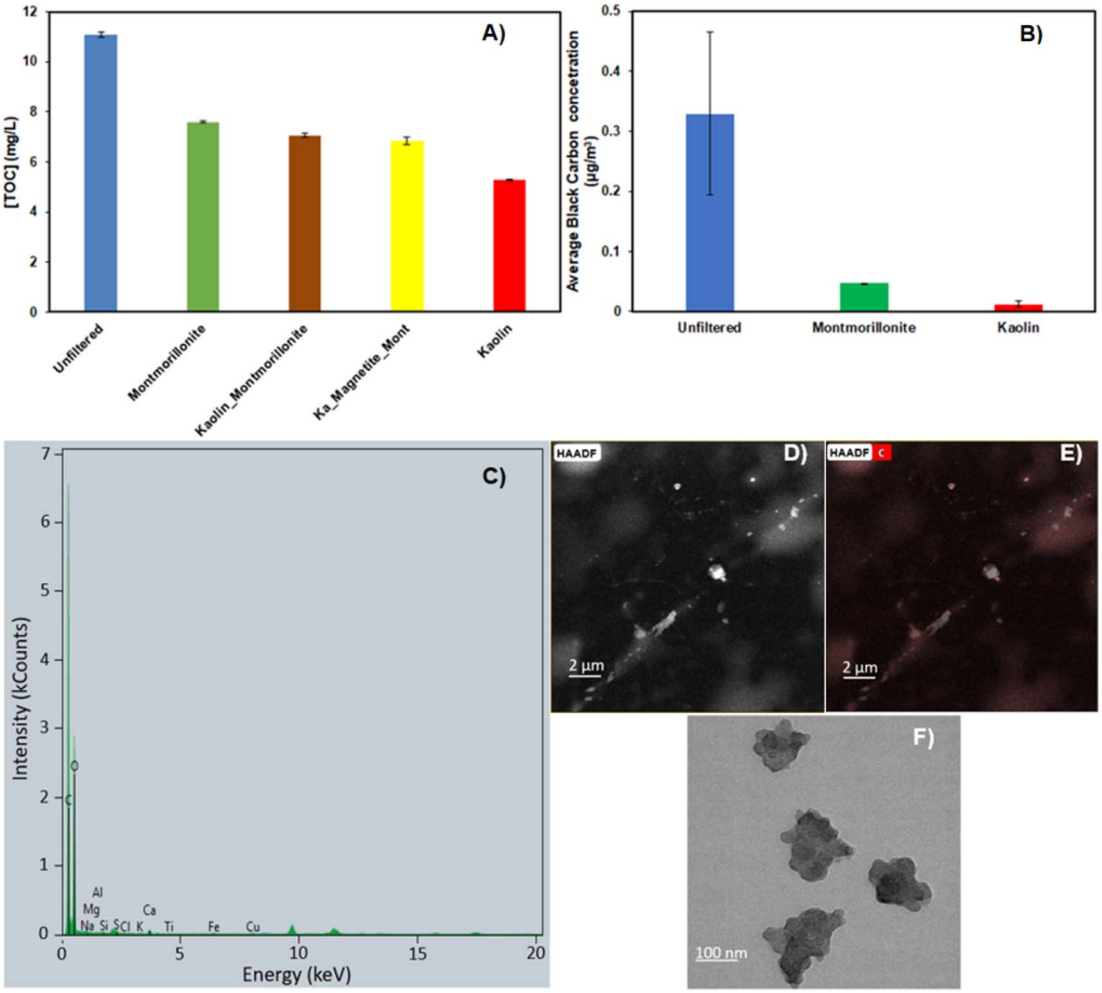

Fig. 2 Total Organic Compound (TOC) and Black Carbon (BC) analysis and high-resolution scanning/transmission electron microscopy (STEM) with energy dispersive X-ray spectroscopy (EDS) results. (A) TOC concentrations for Milli-Q, unfiltered, kaolin-filtered, montmorillonite-filtered, kaolin–montmorillonite-filtered as well as a three layers combo (kaolin–magnetite–montmorillonite)-filtered samples. (B) Photoacoustic Exctintiometer (PAX) determined black carbon mass concentration. (C) EDS results of an unfiltered snow sample. (D) High-angle annular dark-field scanning transmission electron microscopy image of an unfiltered snow sample. (E) Carbon map of the image shown in (D). (F) Bright field scanning/transmission electron microscopy image from an unfiltered snow sample.

sites. This extensive surface area enhances the physical adsorption of hydrophobic molecules like BC through van der Waals forces and hydrophobic interactions at specific sites.[79]

(2) Formation of organoclay:

Clay minerals can swell in aquatic environments, particularly montmorillonite, creating more space between their octahedral and tetrahedral sheets. This swelling allows for the intercalation of organic molecules between the clay layers, resulting in a more hydrophobic environment within the clay structure. This hydrophobic environment is particularly effective in attracting and trapping hydrophobic molecules such as BC.[80]

(3) Cation exchange and hydrophobicity:

Through cation exchange, the clay can replace inorganic ions with more hydrophobic organic ions. It increases the hydrophobic nature of the clay surface, thereby enhancing its ability to adsorb organic compounds like BC.[81]

(4) Aggregation and encapsulation:

The small particle size and high surface area of montmorillonite contribute to the formation of aggregates that can trap hydrophobic molecules like BC within their structure. Once BC particles are trapped within these aggregates, they become effectively encapsulated by the clay mineral, which reduces their mobility and increases their retention.[79]

These mechanisms collectively contribute to the effective removal of BC from snow water by clay minerals, making them an important tool in mitigating the environmental impact of BC on snow and ice-covered surfaces.

3.4.3 Micro/nano plastic analysis: focus on polyethylene glycol and polyethylene. The plastics sector, a crucial part of the chemical industry, manufactures various polymer materials essential for multiple sectors, including packaging, construction, automotive, and consumer products. Market analysis projects that the industry will reach a valuation of 750 billion USD by 2025, propelled by a 5.1% compound annual growth rate (CAGR) from 2020 to 2025.[82] This robust industry also

Open Access Article. Published on 23 September 2024. Downloaded on 2/21/2026 12:45:27 PM.
This article is licensed under a Creative Commons Attribution-NonCommercial 3.0 Unported Licence.

generates substantial waste; in 2019, plastic waste totalled around 353 million tons, a significant increase from 156 million tons in 2000. Alarmingly, it's estimated that 139 million tons of plastic have accumulated in aquatic environments by the same year.[83]

The plastics industry's impact on the environment is significant, accounting for 3.4% of global greenhouse gas emissions, mainly from fossil fuel production and processing. Environmental degradation (factors such as sunlight, oxidation, and physical abrasion) of plastic into micro and nano-plastics is a significant source of air pollution.[50,84–87] These smaller particles are problematic as they can attract and carry toxic substances, posing health risks to marine life and humans, potentially leading to various problems, including physiological stress, suffocation, and reproductive issues. Microplastics have been detected within human tissues, indicating a potential threat to human health as well.[84,88–90]

Polyethylene (PE) and polyethylene glycol (PEG) are among the most used polymers in the plastics industry, with PE being the most prevalent globally. Their widespread use has led to a significant presence of these particles in the air, which can be transferred to snow. Our previous research detailed the occurrence of PE and PEG in snowy environments.[91] Consequently, we focused on exploring clay-based methods for removing these specific particles from snow through an environmentally friendly snow remediation process.

3.5 Focus on polyethylene particles

Considering the widespread presence of polyethylene (PE) in the environment, its adverse health and environmental impact, it became imperative for our study to focus on assessing the efficacy of our remediation process in targeting and removing PE molecules from melted snow water.

We deliberately increased the PE concentration in the test medium to recognize the challenges of detecting PE molecules in snow water and the need for an enhanced understanding of the clay's adsorption capabilities. It was achieved by spiking

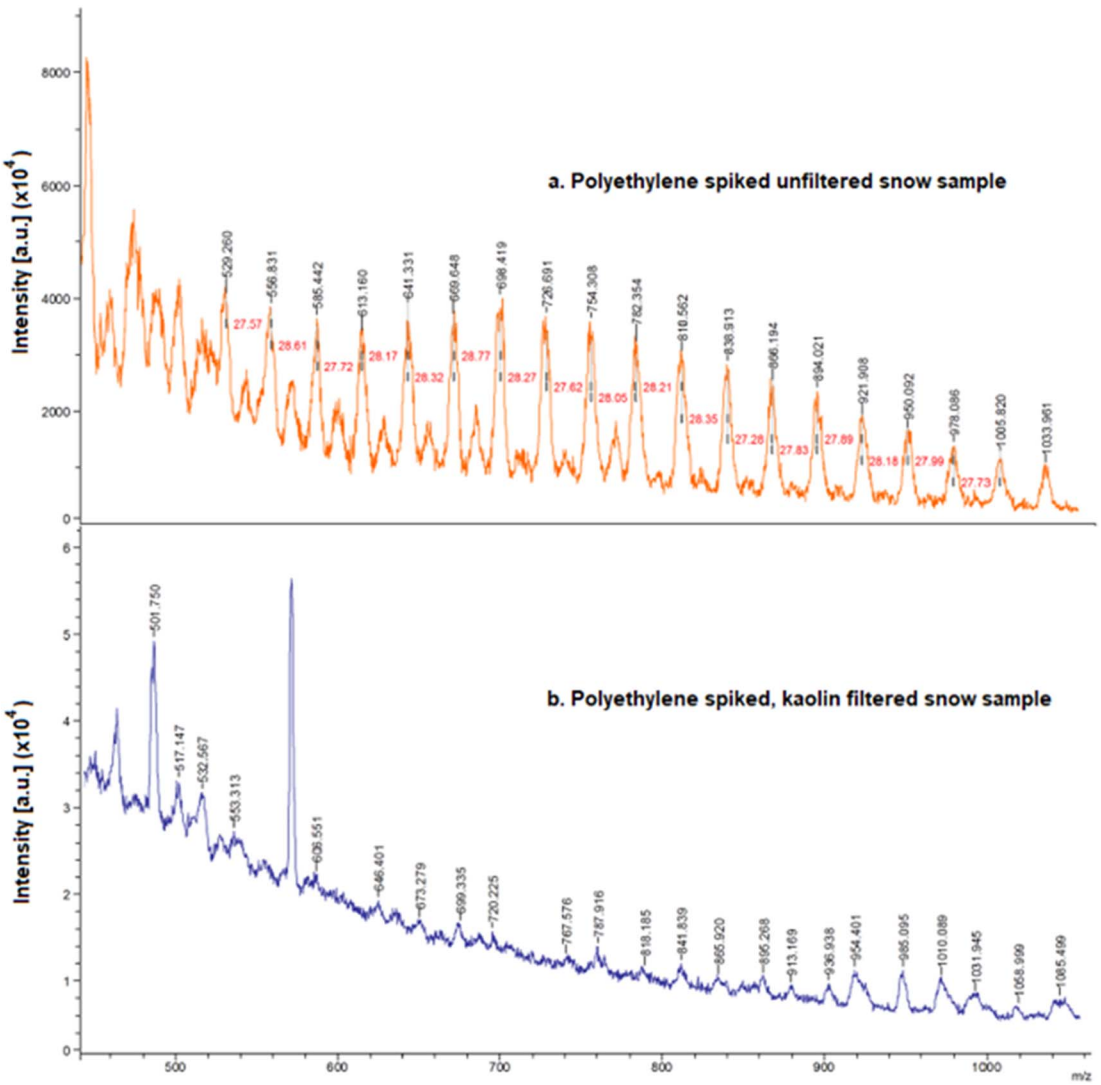

Fig. 3 Nanostructured laser desorption/ionization time-of flight analysis of polyethylene spiked snow water. (a) Accumulation spectrum of a polyethylene spiked unfiltered snow sample. (b) Accumulation spectrum of a polyethylene spiked kaolin filtered snow sample.

© 2024 The Author(s). Published by the Royal Society of Chemistry

Open Access Article. Published on 23 September 2024. Downloaded on 2/21/2026 12:45:27 PM. This article is licensed under a Creative Commons Attribution-NonCommercial 3.0 Unported Licence.

snow water with a toluene-dissolved PE-800 particle solution (10 mg ml^{-1}), increasing the PE concentration. The rationale behind this approach was to simulate a more challenging yet environmentally relevant scenario for PE removal.

Subsequently, we employed Nano-Assisted Laser Desorption/Ionization Mass Spectrometry (NALDI-MS) to analyze the spiked solutions. This technique is particularly suitable for detecting and characterizing polymers like PE due to its higher sensitivity and precision.[25] The resultant NALDI-MS spectrum (Fig. 3a) revealed distinct mass intervals of approximately 28 Da, corresponding to the [–CH_2–CH_2–] repeating units in polyethylene. The next critical phase involved passing the PE-spiked snow water through a kaolin filter. The accumulation spectrum obtained from the kaolin-filtered sample (Fig. 3b) was then meticulously examined. The spectrum lacked the mass intervals associated with PE polymers observed in the unfiltered sample. This absence of PE signatures in the spectrum indicates that the PE concentration post-filtration was below the detection limit of our NALDI-MS methodology (≥100 ng ml^{-1}).[25]

By juxtaposing the spectra obtained before and after kaolin filtration (Fig. 3), we were able to ascertain the clay material's proficiency in targeted PE remediation from snow water. This comparative analysis not only underscores the potential of kaolin as an effective medium for PE removal but also enhances our understanding of its role in environmental remediation processes.

3.6 Focus on polyethylene glycol particles

In this section, we sought to discern the efficacy of clay nanomaterials in filtering out PEG from aqueous snow solutions by comparing the concentrations before and after the remediation process. Like PE analysis, we used an inorganic matrix (ZnO) for the MALDI mass spectrometry technique to enhance the ionization efficiency.

The first phase of our analysis involved constructing a calibration curve for PEG concentrations. To this end, we prepared standard solutions at varying concentrations (0.01, 0.025, 0.05, 0.3, and 0.5 mg l^{-1}). The mass spectrometric analysis of these standards revealed mass intervals consistent with the [–O–CH_2–CH_2–] repeating unit of PEG, thereby validating our methodological approach. Subsequently, we applied the same methodology to analyze raw and filtered snow samples. Using the calibration curve (depicted in Fig. S4†), we determined the concentration of the analyzed samples to be 0.2590, 0.0793, 0.0721 and 0.0018 mg ml^{-1} for unfiltered, montmorillonite-filtered, kaolin-filtered, and kaolin–montmorillonite-filtered samples, respectively. As illustrated in Fig. 4, the results demonstrate the varying degrees of effectiveness of different clay materials in PEG remediation. Notably, while kaolin exhibited superior removal capacity compared to montmorillonite, combining these two clay materials resulted in even more impressive results, with a removal efficiency of up to 99.3%.

This part of our study underscores the potential of clay compounds in snow remediation. It highlights the importance of exploring combinations of different micro/nanomaterials to enhance the efficiency of contaminant removal processes.

3.7 Feasibility analysis of scaling up urban snow disposal remediation strategies

3.7.1 Challenges and innovations in urban snow management: the case of Montreal. Urban centers worldwide face a significant challenge in managing the snowfall they receive, especially given the economic demands and population densities involved. In many cities, snow is cleared from streets and public areas and transported to designated disposal sites. This practice is particularly prevalent in areas with high urban populations, a demographic that has been increasing steadily.

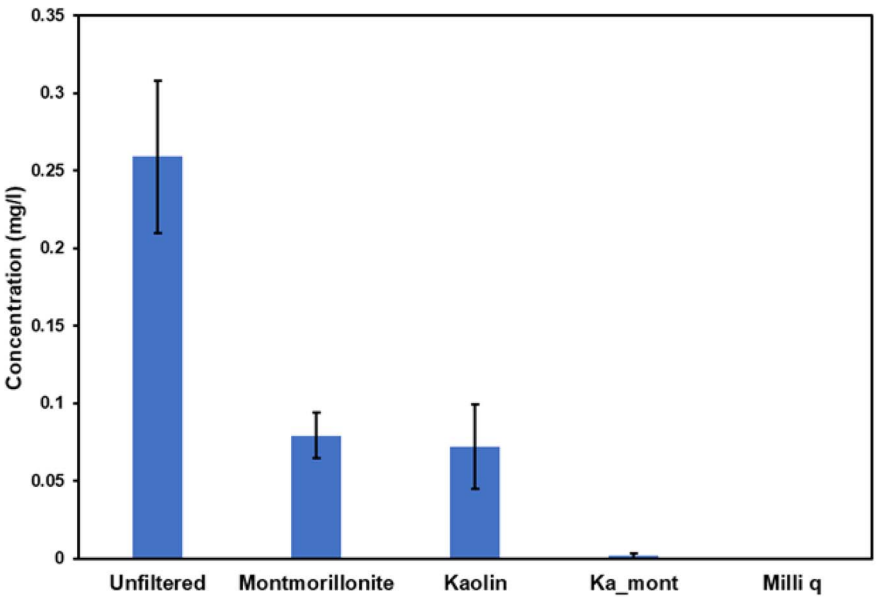

Fig. 4 Determined concentrations of polyethylene glycol by nanostructured laser desorption/ionization time-of flight analysis for unfiltered, 11 μm filter-filtered, montmorillonite-filtered, kaolin-filtered, kaolin–montmorillonite combo (ka_mont)-filtered and Milli-Q samples.

Open Access Article. Published on 23 September 2024. Downloaded on 2/21/2026 12:45:27 PM. This article is licensed under a Creative Commons Attribution-NonCommercial 3.0 Unported Licence.

As of 2018, 55% of the global population resided in urban areas, projected to grow to 68% by 2050.[92] The implications of this growth are substantial, particularly in terms of the potential for snow-mediated pollution to affect a more significant segment of the population.

Montreal serves as a prime example of these challenges. The city, known for its significant snowfall, has established a comprehensive snow management system. As of 2017, Montreal boasted 28 snow disposal sites, including 12 surface sites.[93] These sites play a crucial role in the city's snow management, with the Francon snow depot alone handling about 40% of Montreal's snow.[94] In the 2016–2017 season, these sites collectively managed over 13 million cubic meters of snow, most of which originated from municipal roads and sidewalks.[93]

The disposal process in Montreal is multifaceted. Approximately two-third of the snow is transported to the former Francon quarry pit or 11 dump sites.[93,94] These sites are crucial as they accumulate atmospheric pollution throughout the winter. The remaining one-third of the snow, historically dumped directly into the St. Lawrence River, is managed more sustainably. It is channeled through 16 chutes connected to two large sewage interceptors, akin to metro tunnels, leading to one of the largest wastewater treatment plants in the world.[94]

The latter, innovative approach reflects a growing awareness of the environmental impact of snow disposal. However, with the increasing urban population, especially in areas close to these disposal sites, the need for efficient and environmentally friendly snow disposal methods has become more pressing. Montreal's weather data from 2023 illustrates the scale of this challenge: the city received about 220.6 cm of snow,[95] covering an area of 4670.1 square kilometers, with a population density of 919.0 people per square kilometer.[96] This high density

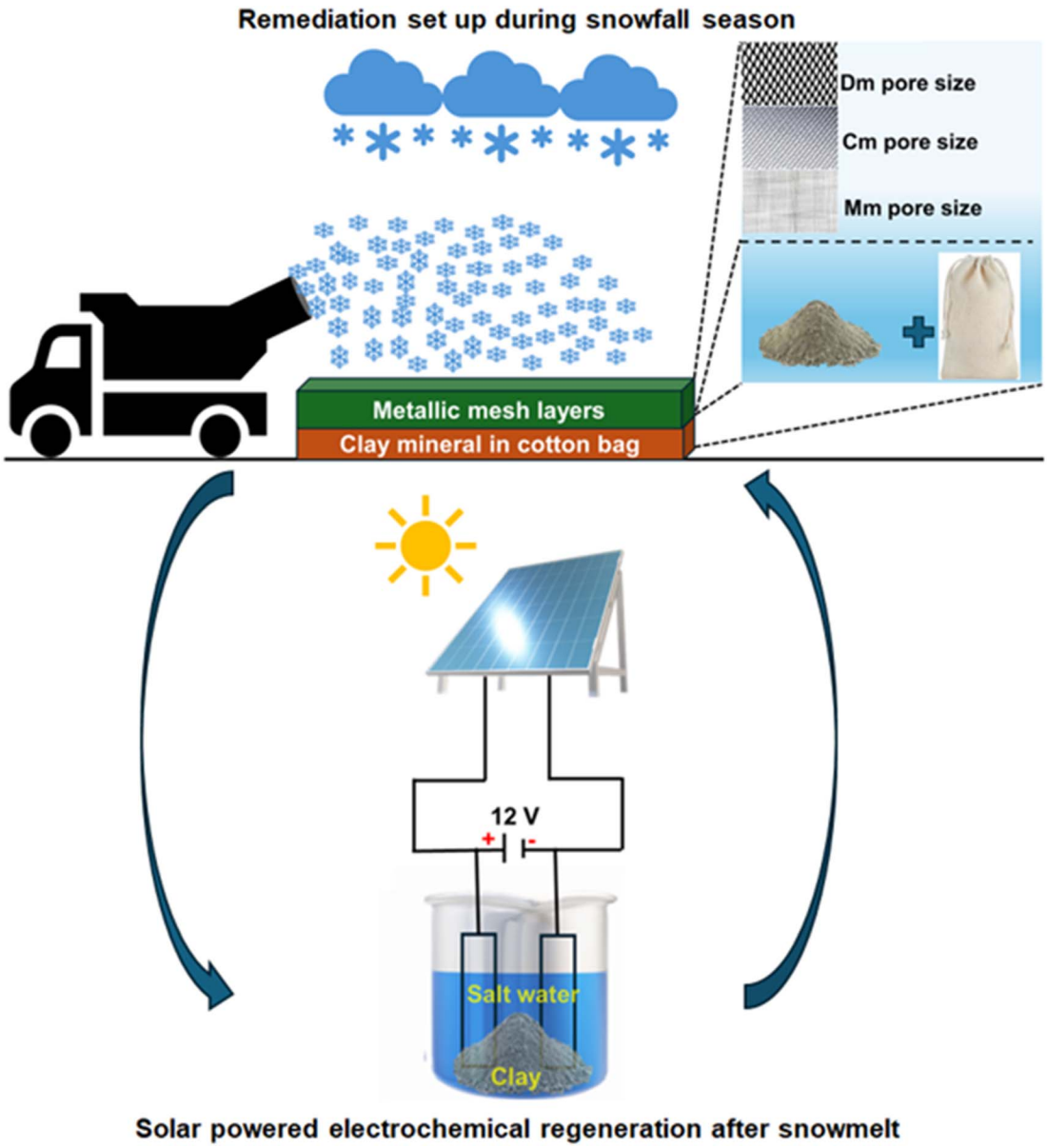

Fig. 5 Simplified suggested setup for snow remediation at disposal sites.

© 2024 The Author(s). Published by the Royal Society of Chemistry

Open Access Article. Published on 23 September 2024. Downloaded on 2/21/2026 12:45:27 PM. This article is licensed under a Creative Commons Attribution-NonCommercial 3.0 Unported Licence.

underscores the potential for significant snow-related pollution, necessitating targeted reduction strategies at major disposal sites.

3.7.2 Clay mineral centered snow remediation as an economic and sustainable option. In this study, two types of clay minerals, kaolin and montmorillonite (the main component of bentonite), were found to be efficient interfaces for the uptake of contaminants in snow. In addition to their high adsorption efficiency, these clays are economically attractive due to their relatively low cost. For instance, the average export price of one ton of kaolin in 2022 in Canada was $147,[97] whereas 1 ton of bentonite was priced at $366 in 2023.[98]

A proposed solution for mitigating this pollution involves a sophisticated, multi-layered filtration system. This system consists of metal meshes and cotton bags filled with clay minerals to capture and adsorb pollutants from the snow, as depicted in Fig. 5. The metal meshes are intended to trap larger debris and contaminants, while the clay minerals in the cotton bags target smaller, micro-sized particles. This setup remains in place throughout the winter, from the first snowfall to the final thaw.

Post-thaw, the clay-filled cotton bags will be collected for on-site regenerative treatment. Using solar-powered electrodeposition (ensuring a zero-net energy process), most of the metallic elements adsorbed by the clay can be effectively removed, restoring the clay's adsorption capacity. The proposed system is expected to have minimal environmental impact, as the clay powder is securely contained within the cotton bags. This design allows for easy retrieval of the bags during the summer. The regenerated clay can then be reused for the following winter season. In cases where the clay needs to be discarded, the use of bags simplifies collection and ensures proper disposal.

This process was tested in a laboratory setting using montmorillonite clay. After absorbing contaminants from the snow, the clay underwent electrolysis (the voltage set to 12 V for 10 g of clay mineral in 200 ml of Milli-Q water) in a saltwater solution (by dissolving 4 g of NaCl in the water solution), with either copper (a simple wire was used) or graphite (isolated from a pencil) electrodes. The results were promising (Table S1†), showing that a large portion of the metal contaminants could be removed, thus effectively regenerating the clay. In this study, we successfully carried out the regeneration process using electrochemical methods, specifically electrodeposition on electrodes, with a primary focus on metallic contaminants. We recommend future studies to explore additional regeneration methods for addressing organic matter, thereby broadening the scope of our research.

Implementing this system on a larger scale poses several challenges, including the need to adapt to Montreal's extremely low winter temperatures and the prolonged exposure of clay at disposal sites, which may affect the efficiency of the remediation process. However, in cold-climate cities like Montreal, where frequent precipitation, deposition, and melting occur, contaminants are periodically exposed to the clay mineral surfaces. We can ensure adequate exposure of pollutants to the clay surfaces by utilizing several layers of bags. Additionally, since temperatures in Montreal typically remain below zero for extended periods during winter, processes like the evaporation of contaminants (gaseous and aerosol) are minimized, keeping them trapped in the snow matrix for longer. In other cities with periodic snowfall, more frequent recycling of the clay minerals may be required. We aim to further enhance the system's cost-effectiveness as we scale it up. The next step in this technology includes adapting the existing setup to specific sites and meteorological conditions to improve its recycling capacities and save costs. This research is a foundational step for refining and improving the process in future projects.

Despite the challenges, the preliminary laboratory results are encouraging, suggesting that this method could be a viable solution for reducing pollution at snow disposal sites. As urban populations continue to grow and environmental concerns become increasingly pressing, such innovative snow management approaches are desirable and essential. They represent a proactive step toward sustainable urban living, balancing the practical needs of snow removal with the imperative to protect and preserve the urban environment now and in future.

4 Concluding remarks

We developed an innovative snow contaminant remediation technique using clay materials, successfully filtering various contaminants from snow. A suite of diverse analytical techniques and methods confirmed its effectiveness in removing a broad range of organic and inorganic molecules and particulate matter such as black carbon. This technology significantly lowered the Mean Freezing Temperature (MFT) from −11 to −17 °C, indicating improved snow purity. Elemental analysis through ICP-MS/MS revealed that over 95% of metals were removed, while NALDI-MS analysis showed more than 99% reduction in polyethylene glycol (PEG) and polyethylene (PE) particles. Furthermore, >97% of black carbon and over 50% of organic carbon were eliminated. This sustainable and inexpensive technology is promising for removing nano- and micro-contaminants and larger particles from snow. This technology can be an added value to current snow remediation practices in urban sites.

This technology can decrease the re-emission of contaminants in air, soil, and water leaching upon the melting process, which will allow the improvement of urban ecosystems by reducing nano and microparticles in snow and help mitigate human exposure to pollutants. Most humans live in cities, and most energy is used in cities. It is essential for cities that receive periodical or permanent snow to advance their existing system, using zero-net energy technologies of the future, including this clay-mineral system. It is already known that snow contaminants can change the composition and the radiation of snow.[16,99] Therefore, we recommend further research on snow biogeochemistry and climate interactions for cold urban cities.

Data availability

The data used to support the findings of this study are included within the article and the ESI.†

Open Access Article. Published on 23 September 2024. Downloaded on 2/21/2026 12:45:27 PM. This article is licensed under a Creative Commons Attribution-NonCommercial 3.0 Unported Licence.

Conflicts of interest

There are no conflicts to declare.

Acknowledgements

We are grateful to the Natural Science and Engineering Research Council of Canada (NSERC), the Canadian Foundation for innovation (CFI), Prima Quebec, PO-Labs, and CREATE PURE. We also thank Mr Saade and Ms Zi Wang for insightful helps.

References

1 P. Huybrechts, in *Encyclopedia of Paleoclimatology and Ancient Environments*, 2009, pp. 221–226.
2 D. Riseborough, O. Anisimov, C. Guodong, V. J. Lunardini, M. Gavrilova, E. A. Köster, R. M. Koerner and M. F. Meier, *Climate Change: The IPCC Impacts Assessment, Report prepared for the Intergovernmental Panel on Climate Change by Working Group II*, ed. W. J. M. Tegart, G. W. Sheldon and D. C. Griffiths, Australian Government Publishing Service, Canberra, 1990, ch. 7, pp. 1–33.
3 R. Mott, V. Vionnet and T. Grünewald, *Front. Earth Sci.*, 2018, **6**, 197.
4 S. G. Warren and W. J. Wiscombe, *J. Atmos. Sci.*, 1980, **37**, 2734–2745.
5 R. Rangel-alvarado, H. Li and P. A. Ariya, *Environ. Sci.*, 2022, 891–920, DOI: **10.1039/d2ea00067a**.
6 M. G. Flanner, M. Barlage, D. K. Perovich, M. A. Tschudi and K. Shell, *Nat. Geosci.*, 2011, **4**, 151–155.
7 R. P. Gupta, U. K. Haritashya and P. Singh, *Rem. Sens. Environ.*, 2005, **97**, 458–469.
8 R. P. Gupta, *Encyclopedia of Snow, Ice and Glaciers*, 2014, pp. 241–242.
9 S. Bokhorst, S. H. Pedersen, L. Brucker, O. Anisimov, J. W. Bjerke, R. D. Brown, D. Ehrich, R. L. H. Essery, A. Heilig, S. Ingvander, C. Johansson, M. Johansson, I. S. Jónsdóttir, N. Inga, K. Luojus, G. Macelloni, H. Mariash, D. McLennan, G. N. Rosqvist, A. Sato, H. Savela, M. Schneebeli, A. Sokolov, S. A. Sokratov, S. Terzago, D. Vikhamar-Schuler, S. Williamson, Y. Qiu and T. V. Callaghan, *Ambio*, 2016, **45**, 516–537.
10 J. Dozier and T. H. Painter, *Annu. Rev. Earth Planet. Sci.*, 2004, **32**, 465–494.
11 M. Matiu, A. Crespi, G. Bertoldi, C. Maria Carmagnola, C. Marty, S. Morin, W. Schöner, D. Cat Berro, G. Chiogna, L. De Gregorio, S. Kotlarski, B. Majone, G. Resch, S. Terzago, M. Valt, W. Beozzo, P. Cianfarra, I. Gouttevin, G. Marcolini, C. Notarnicola, M. Petitta, S. C. Scherrer, U. Strasser, M. Winkler, M. Zebisch, A. Cicogna, R. Cremonini, A. Debernardi, M. Faletto, M. Gaddo, L. Giovannini, L. Mercalli, J. M. Soubeyroux, A. Sušnik, A. Trenti, S. Urbani and V. Weilguni, *Cryosphere*, 2021, **15**, 1343–1382.
12 L. Bengtsson and A. Semadeni-Davies, *Encyclopedia of Snow, Ice and Glaciers*, 2014, pp. 1211–1217.
13 R. Rangel-alvarado, H. Li and P. A. Ariya, *Environ. Sci.*, 2022, 891–920, DOI: **10.1039/d2ea00067a**.
14 D. Pal, A. Dastoor and P. A. Ariya, *Urban Clim.*, 2020, **34**, 100713.
15 H. Lee, U. Kurien and P. A. Ariya, *J. Phys. Chem. A*, 2022, **126**, 6953–6962.
16 Y. Nazarenko, R. B. Rangel-Alvarado, G. Kos, U. Kurien and P. A. Ariya, *Environ. Sci. Pollut. Res.*, 2017, **24**, 4480–4493.
17 Y. Nazarenko and P. A. Ariya, *Atmosphere*, 2021, **12**, 10–13.
18 R. B. Rangel-Alvarado, C. E. Willis, J. L. Kirk, V. L. St Louis, M. Amyot, D. Bélanger and P. A. Ariya, *Environ. Pollut.*, 2019, **252**, 289–295.
19 C. E. Willis, J. L. Kirk, V. L. St Louis, I. Lehnherr, P. A. Ariya and R. B. Rangel-Alvarado, *Environ. Sci. Technol.*, 2018, **52**, 531–540.
20 G. Kos and P. A. Ariya, *Anal. Bioanal. Chem.*, 2006, **385**, 57–66.
21 R. Mortazavi, S. Attiya and P. A. Ariya, *Sci. Total Environ.*, 2019, **690**, 277–289.
22 M. F. Rahim, D. Pal and P. A. Ariya, *Environ. Pollut.*, 2019, **246**, 734–744.
23 I. Kasprzyk and K. Borycka, *Int. J. Biometeorol.*, 2019, 1651–1658.
24 M. Ganguly and P. A. Ariya, *ACS Earth Space Chem.*, 2019, **3**, 1729–1739.
25 Z. Wang, N. K. Saadé and P. A. Ariya, *Environ. Pollut.*, 2021, 116698, DOI: **10.1016/j.envpol.2021.116698**.
26 H. I. Abdel-shafy and M. S. M. Mansour, *Egypt. J. Pet.*, 2016, **25**, 107–123.
27 P. A. Ariya, J. F. Hopper and G. W. Harris, *J. Atmos. Chem.*, 1999, **34**, 55–64.
28 T. Meyer, Y. D. Lei and F. Wania, *Water Res.*, 2010, **45**, 1147–1156.
29 G. Kos, V. Kanthasami and P. A. Ariya, *Environ. Sci.: Processes Impacts*, 2014, 2592–2603.
30 P. A. Ariya, F. Domine, G. Kos, M. Amyot, V. Côté, H. Vali, T. Lauzier, W. F. Kuhs, K. Techmer, T. Heinrichs and R. Mortazavi, *Environ. Chem.*, 2011, **8**, 63–73.
31 G. Kos and P. A. Ariya, *J. Geophys. Res. C Oceans Atmos.*, 2010, **115**, 1–14.
32 R. Mortazavi, S. Attiya and P. A. Ariya, *Atmos. Chem. Phys.*, 2015, 6183–6204.
33 P. A. Ariya, G. Kos, R. Mortazavi, E. D. Hudson, V. Kanthasamy, N. Eltouny, J. Sun and C. Wilde, *Atmospheric and Aerosol Chemistry*, 2014, vol. 339, pp. 145–199.
34 V. Côté, G. Kos, R. Mortazavi and P. A. Ariya, *Sci. Total Environ.*, 2007, **390**, 2–3.
35 H. A. Al-Abadleh, *Atmospheric Aerosol Chemistry*, 2022.
36 R. Mortazavi, C. T. Hayes and P. A. Ariya, *Environ. Chem.*, 2008, **5**, 373–381.
37 A. Steffen, T. Douglas, M. Amyot, P. Ariya, K. Aspmo, T. Berg, J. Bottenheim, S. Brooks, F. Cobbett, A. Dastoor, A. Dommergue, R. Ebinghaus, C. Ferrari, K. Gardfeldt, M. E. Goodsite, D. Lean, A. J. Poulain, C. Scherz, H. Skov, J. Sommar and C. Temme, *Atmos. Chem. Phys.*, 2008, **8**, 1445–1482.

© 2024 The Author(s). Published by the Royal Society of Chemistry

Open Access Article. Published on 23 September 2024. Downloaded on 2/21/2026 12:45:27 PM. This article is licensed under a Creative Commons Attribution-NonCommercial 3.0 Unported Licence.

38 D. Voisin, J. L. Jaffrezo, S. Houdier, M. Barret, J. Cozic, M. D. King, J. L. France, H. J. Reay, A. Grannas, G. Kos, P. A. Ariya, H. J. Beine and F. Domine, *J. Geophys. Res. C Oceans Atmos.*, 2012, **117**, 1–17.
39 H. Li and P. A. Ariya, *J. Geophys. Res.: Atmos.*, 2021, JD035265, DOI: 10.1029/2021JD035265.
40 Z. Wang, A. Pilechi, F. M. Cheung and P. A. Ariya, *Water Res.*, 2023, **235**, 10.
41 J. Kaur, M. Ganguly, R. Rangel-Alvardo, D. Pal, R. Hall and P. A. Ariya, *ACS Earth Space Chem.*, 2022, **6**, 2236–2249.
42 Y. Nazarenko, S. Fournier, U. Kurien, R. B. Rangel-Alvarado, O. Nepotchatykh, P. Seers and P. A. Ariya, *Environ. Pollut.*, 2017, **223**, 665–675.
43 Q. Deng, L. Deng, Y. Miao, X. Guo and Y. Li, *Environ. Res.*, 2019, **169**, 237–245.
44 P. L. Kinney, *Curr. Environ. Health Rep.*, 2018, **5**, 179–186.
45 R. J. Delfino, C. Sioutas and S. Malik, *Environ. Health Perspect.*, 2005, 934–946.
46 World Health Organization, *7 Million Premature Deaths Annually Linked to Air Pollution*, 2014.
47 World Health Organization, *Household Air Pollution*, 2022.
48 World Health Organization, *Ambient (Outdoor) Air Pollution*, 2022.
49 Z. A. Kanji, L. A. Ladino, H. Wex, Y. Boose, M. Burkert-Kohn, D. J. Cziczo and M. Krämer, *Meteorol. Monogr.*, 2017, **58**, 1.1–1.33.
50 K. Enders, R. Lenz, C. A. Stedmon and T. G. Nielsen, *Mar. Pollut. Bull.*, 2015, **100**, 70–81.
51 M. Senior, R. Scheckenberger and R. Moore, *16th International Environmental Specialty Conference 2018, Held as Part of the Canadian Society for Civil Engineering Annual Conference 2018*, 2019, pp. 31–38.
52 C. Jiang, J. Li, H. Li, Y. Li and L. Chen, *Water, Air, Soil Pollut.*, 2017, 468, DOI: 10.1007/s11270-017-3636-6.
53 G. T. Blecken, Y. Zinger, A. Deletić, T. D. Fletcher and M. Viklander, *Ecol. Eng.*, 2009, **35**, 769–778.
54 Md. A. Ali and N. B. Pickering, *J. Sustain. Water Built Environ.*, 2022, **9**(1), DOI: 10.1061/jswbay.0001004.
55 J. Wolfand, C. J. Poor, B. L. H. Taylor, E. Morrow, A. Radke and E. Diaz-Gunning, *J. Environ. Eng.*, 2023, **149**, 1–10.
56 D. Liu, J. J. Sansalone and F. K. Cartledge, *J. Environ. Eng.*, 2005, **131**, 1178–1186.
57 F. Qiu, H. Lv, X. Zhao and D. Zhao, *Int. J. Environ. Res. Publ. Health*, 2019, **16**, 1–15.
58 A. Matilainien, M. Vepsalainen and M. Sillanpaa, *Adv. Colloid Interface Sci.*, 2010, 189–197.
59 F. Nakazawa and K. Goto-Azuma, *J. Glaciol.*, 2022, **68**, 166–173.
60 M. Simonič, *Membranes*, 2021, 976, DOI: 10.3390/membranes11120976.
61 R. B. Rangel-alvarado, Y. Nazarenko and P. A. Ariya, *J. Geophys. Res.: Atmos.*, 2015, **120**, 11760–11774.
62 D. W. O'Connell, C. Birkinshaw and T. F. O'Dwyer, *Bioresour. Technol.*, 2008, **99**, 6709–6724.
63 J. Briffa, E. Sinagra and R. Blundell, *Heliyon*, 2020, **6**, e04691.
64 H. Ramírez-Malule, D. H. Quiñones-Murillo and D. Manotas-Duque, *Emerging Contam.*, 2020, **6**, 179–193.
65 Y. Nazarenko and P. A. Ariya, *Atmosphere*, 2021, **12**, 10–13.
66 M. F. Brigatti, E. N. Galan and B. K. G. Theng, in *Developments in Clay Science*, 2013, pp. 21–57.
67 M. K. Uddin, *Chem. Eng. J.*, 2017, **308**, 438–462.
68 F. Bergaya and G. Lagaly, *Dev. Clay Sci.*, 2006, **1**, 1–18.
69 F. Bergaya and G. Lagaly, in *Handbook of Clay Science*, 2006.
70 B. Chu, J. Hao, H. Takekawa, J. Li, K. Wang and J. Jiang, *Atmos. Environ.*, 2012, **55**, 26–34.
71 B. Chu, J. Liggio, Y. Liu, H. He, H. Takekawa, S. M. Li and J. Hao, *Sci. Rep.*, 2017, **7**, 1–9.
72 N. Lee, P. J. Schuck, P. S. Nico and B. Gilbert, *J. Phys. Chem. Lett.*, 2015, **6**, 970–974.
73 E. Tombácz, I. Y. Tóth, D. Nesztor, E. Illés, A. Hajdú, M. Szekeres and L. Vékás, *Colloids Surf., A*, 2013, **435**, 91–96.
74 S. G. Muntean, M. A. Nistor, E. Muntean, A. Todea, R. Ianoș and C. Păcurariu, *J. Chem.*, 2018, 1–16, DOI: 10.1155/2018/6249821.
75 G. D. Yuan, B. K. G. Theng, J. Churchman and W. P. Gates, *Dev. Clay Sci.*, 2013, 591–604.
76 H. Zhang and Z. Wang, *Adv. Clim. Change Res.*, 2011, **2**, 23–30.
77 J. Ström, J. Svensson, H. Honkanen, E. Asmi, N. B. Dkhar, S. Tayal, V. P. Sharma, R. Hooda, O. Meinander, M. Leppäranta, H. W. Jacobi, H. Lihavainen and A. Hyvärinen, *Elementa*, 2022, **10**, 1–15.
78 M. Réveillet, M. Dumont, S. Gascoin, M. Lafaysse, P. Nabat, A. Ribes, R. Nheili, F. Tuzet, M. Ménégoz, S. Morin, G. Picard and P. Ginoux, *Nat. Commun.*, 2022, **13**, 1–12.
79 F. Bergaya and G. Lagaly, *Dev. Clay Sci.*, 2006, **1**, 1–18.
80 L. Betega de Paiva, A. R. Morales and F. R. Valenzuela Díaz, *Appl. Clay Sci.*, 2008, **42**, 8–24.
81 A. Awad, S. M. R. Shaikh, R. Jalab, M. H. Gulied, M. S. Nasser, A. Benamor and S. Adham, *Sep. Purif. Technol.*, 2019, **228**, 1–39.
82 M. R. Arc Industry, *Polymers Market – Forecast(2023–2028)*, 2023.
83 OECD, *Global Plastics Outlook: Economic Drivers, Environmental Impacts and Policy Options*, Paris, 2022.
84 A. Chamas, H. Moon, J. Zheng, Y. Qiu, T. Tabassum, J. H. Jang, M. Abu-Omar, S. L. Scott and S. Suh, *ACS Sustainable Chem. Eng.*, 2020, **8**, 3494–3511.
85 W. Zhang, Z. Dong, L. Zhu, Y. Hou and Y. Qiu, *ACS Nano*, 2020, **14**, 7920–7926.
86 T. Hu, P. He, Z. Yang, W. Wang, H. Zhang, L. Shao and F. Lü, *Sci. Total Environ.*, 2022, **828**, 154400.
87 S. Herath, D. Hagare, Z. Siddiqui and B. Maheshwari, *Environ. Monit. Assess.*, 2022, 173, DOI: 10.1007/s10661-022-09849-1.
88 J. Hwang, D. Choi, S. Han, S. Y. Jung, J. Choi and J. Hong, *Sci. Rep.*, 2020, **10**, 1–12.
89 R. Geyer, J. R. Jambeck and K. L. Law, *Sci. Adv.*, 2017, **3**, 25–29.
90 M. T. Nuelle, J. H. Dekiff, D. Remy and E. Fries, *Environ. Pollut.*, 2014, **184**, 161–169.
91 Z. Wang, N. K. Saadé and P. A. Ariya, *Environ. Pollut.*, 2021, 116698, DOI: 10.1016/j.envpol.2021.116698.

© 2024 The Author(s). Published by the Royal Society of Chemistry

Open Access Article. Published on 23 September 2024. Downloaded on 2/21/2026 12:45:27 PM.
This article is licensed under a Creative Commons Attribution-NonCommercial 3.0 Unported Licence.

92 United Nations, Department of Economic and Social Affairs (DESA), 68% of the World Population Projected to Live in Urban Areas by 2050, Says UN, 2018.
93 C. Michele, *Galipeau CPA Auditor, Report of the auditor general of the ville de Montreal. Section 4.4: Snow Management*, Montreal, 2017.
94 P. F. Trent, *Montreal Gazette*, 2024.
95 *Montréal Historical Snowfall*, **https://montreal.weatherstats.ca/metrics/snow.html**, accessed 1 February 2024.
96 S. Canada, *Statistics Canada: Focus on Geography Series, 2021 Census of Population*. Montréal, Census metropolitan area, **https://www12.statcan.gc.ca/census-recensement/2021/as-sa/fogs-spg/Page.cfm?lang=e&topic=1&dguid=2021S0503462**, accessed 1 February 2024.
97 *Canada – Kaolin – Market Analysis, Forecast, Size, Trends and Insights*, **https://www.indexbox.io/search/kaolin-price-canada/**, accessed 1 February 2024.
98 *Canada – Bentonite – Market Analysis, Forecast, Size, Trends and Insights*, **https://www.indexbox.io/search/bentonite-price-canada/**, accessed 23 February 2024.
99 Y. Nazarenko, U. Kurien, O. Nepotchatykh, R. B. Rangel-alvarado and P. A. Ariya, *Environ. Sci.: Processes Impacts*, 2016, 190–199.

© 2024 The Author(s). Published by the Royal Society of Chemistry